

Piotr SZCZERBA
Paweł RZUCIDŁO
Zygmunt SZCZERBA
Grzegorz DRUPKA

VISION SYSTEM SUPPORTING THE PILOT IN VARIABLE LIGHT CONDITIONS

UKŁAD WIZYJNY WSPOMAGAJĄCY PILOTA W WARUNKACH ZMIENNEGO OŚWIETLENIA*

The aim of this study is to demonstrate the applicability of contemporary optoelectronic systems supported by image processing algorithms in aviation. Optoelectronic systems can support the pilot's work or the work of an Unmanned Aerial Vehicle (UAV) operator after being installed in the cockpit of the pilot or in a ground station. The origin of the problem is related to the aspects of safe operation of the aircraft in the conditions of dynamically changing ambient light observed by the aircraft pilot or operator monitoring the monitor at the ground station and observing the image from the camera installed on the UAV. The proposed solution is to help avoid situations in which the pilot's/operator's situational awareness deteriorates due to strong optical phenomena.

Keywords: *indicator, pilot, operator, ground station, UAV operation, optical phenomena, vision algorithms, adaptive algorithms, reliability of operations.*

Celem niniejszego opracowania jest zademonstrowanie możliwości zastosowania współczesnych układów optoelektronicznych wspomaganých przez algorytmy przetwarzania obrazu w lotnictwie. Układy optoelektroniczne mogą wspomóc pracę pilota lub pracę operatora bezzałogowego statku powietrznego (BSP) po zainstalowaniu w kabinie pilota bądź w stacji naziemnej. Geneza problemu jest związana z aspektami bezpiecznej eksploatacji statku powietrznego w warunkach dynamicznie zmieniającego się oświetlenia otoczenia obserwowanego przez pilota samolotu lub operatora śledzącego monitor w stacji naziemnej i obserwującego obraz z kamery zainstalowanej na BSP. Zaproponowane rozwiązanie ma pomóc uniknąć sytuacji, w których świadomość sytuacyjna pilota/operatora pogarsza się na skutek silnych zjawisk optycznych.

Słowa kluczowe: *wskaźnik, pilot, operator, stacja naziemna, eksploatacja UAV, zjawiska optyczne, algorytmy wizyjne, algorytmy adaptacyjne, niezawodność operacji.*

1. Introduction

The pilot - aircraft layout is one of the more complex anthropo-technological system [10, 30, 32, 43]. The main reason for making mistakes by pilots is the large amount of information received in a small period of time [14, 15, 29, 30]. A characteristic feature of the pilot's work is the transfer of attention to instruments and simultaneous interpolation of information from incoming signals [6, 16, 29, 43]. This involves a number of risks that can lead to a chain of dangerous events that could pose a threat to the health and life of the crew and passengers [10, 30, 38]. Appropriate cabin equipment, optimizes the division of functions between the operator and the machine, minimizing the hazards. The cab should be characterized by proper adaptation of the remote control to the machine and vice versa [41, 43]. The pilot of the aircraft, or the operator of the unmanned aircraft, performs actions based on the received situational information [5, 15, 32]. With full information, he is able to do his job properly. The problem starts when there are disturbances of the received signals or there is a complete lack of them. This may be important in relation to the readings of on-board instruments, but also to information received directly from the environment. An example of an accident in which the choice of land for emergency landing took place was on 22/03/2014 from the Kaniów EPKW to Mielec EPML airport. Because the landing took

place under the sun, the crew noticed only a dozen meters above the ground that the field was divided by a plowed belt of ground. There was a touchdown, and the plane overturned [31].

This study deals with the concept of a solution that minimizes interference and artefacts [40] due to overexposures caused by strong sunlight and sources of artificial lighting (eg. a laser beam directed towards the pilot's cabin) [26]). During the operation of the aircraft, the phenomenon of glare is particularly dangerous. This problem also occurs in other means of transport. The unquestionable inspirations, in this field of research are scientific works conducted in the automotive industry. Extensive research, including implementations, has been presented in the works [11, 19, 45] and concern the improvement of traditional blinds for drivers and the optoelectronic filter within the windshield [9, 47]. Research on the effect of glare on drivers from the rear-view mirror during night driving presents the work [48]. The latest solutions of matrix lights eliminating the problem of dazzle from headlamps, enabling independent dynamic control of multiple light beams of the car are presented in the works [22, 23, 37, 49].

In aviation, visual orientation is important in both piloting and navigation [42]. It also allows to avoid collisions with other aircraft. The problem of dazzle, does not only concern manned aviation, it is also present in unmanned aviation. It is mainly related to interference from sunlight, but also from amateur lasers. The most commonly

(*) Tekst artykułu w polskiej wersji językowej dostępny w elektronicznym wydaniu kwartalnika na stronie www.ein.org.pl

used method of limiting effects of dazzle during the operation of the aircraft are safety goggles, elimination of shiny surfaces or covering of radiation sources (Fig. 1) [2, 34, 35, 41, 45]. The disadvantages of such solutions include:

- the use of screens of geometric blinds adapted to the glass and plane,
- engaging the pilot for the manual setting of the shutters,
- operation in a limited area of the aircraft window,
- the occurrence of side disturbances and artifacts in the border areas of the blinds,
- procedural ban on the use of blinds during take-off and landing,
- limited use in unmanned aviation.



Fig. 1. The interior of the Boeing 737 cabin; unprotected window from the first officer's side (left) and window from the side of the captain's chair, partially covered by the shutter (own study)

Glasses are an effective tool to protect the eyesight, however, due to the variety and specificity of filters, they can impair the reliability of reading information from on-board instruments [36]. Current research conducted in the world, in the aspect of improving the vision of pilots, is mainly related to ergonomics and improvements in the information economy. They concern, among others the development of augmented reality as well as systems of synthetic [24] and enhanced vision [18, 25]. Strengthened vision systems use technologies related to infrared observation and radiolocation [4, 7, 12, 13, 28]. These systems allow for direct observation of the surroundings and runway during night or fog landing. The pilot, thanks to the use of this class of systems, sees objects that can be a potential threat. The motivation for undertaking work on a system supporting the pilot in the conditions of variable lighting is the disproportion of existing solutions in this area, relative to systems related to supporting night vision and operations performed in difficult weather conditions.

2. A vision system as a support tool for a pilot or UAV operator

2.1. The concept of the proposed solution

The pilot-operator support video system proposed in this paper allows observation of the environment on a specially designed module installed in the aircraft cabin (or in a ground station in the case of the UAV system). The vision system is designed to process the image so as to "pull out" the key information for the pilot, and in addition to enable the visualization of the observed environment without disturbances, with the simultaneous possibility of indicating potential threats (eg. animals on the runway). Fig. 2 presents a schematic diagram of a system that is a combination of four parts: the optics and image transducer, the acquisition system, the image processing system captured (vision algorithm) and the visualization system of the final image.

Fig. 3 presents a simplified diagram presenting a one-dimensional control system presenting the aircraft pilot control process (or unmanned aerial vehicle by the operator of a ground station). The human-aircraft system is presented in a simplified way, as only visual stimuli are taken into account. These stimuli come to the pilot from on-board instruments, as well as from the image seen through the win-

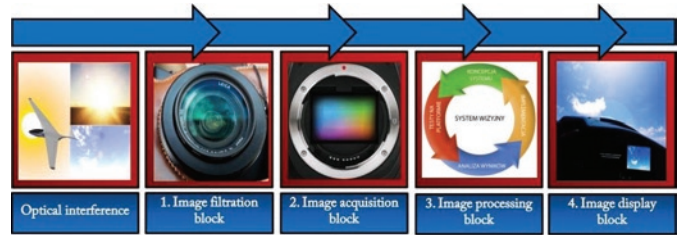


Fig. 2. Schematic diagram of the adaptive vision system (own elaboration)

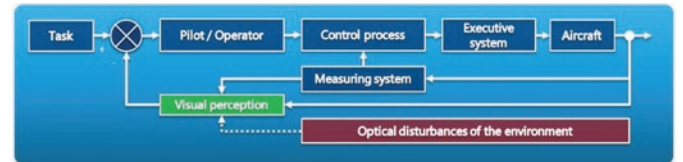


Fig. 3. Diagram of aircraft control process taking into account the influence of optical interference

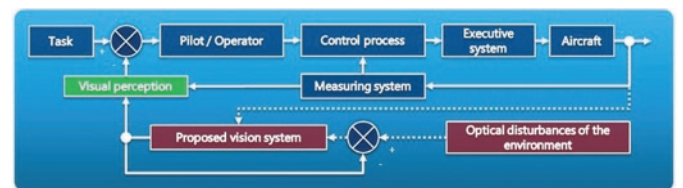


Fig. 4. A simplified scheme of the aircraft control process in case of optical interference, taking into account the presence of the proposed vision system

dow of the aircraft cabin (in the case of the pilot). In the case of the UAV operator stimuli come from the screen of the monitor being an element of ground station devices. Based on Fig. 3, the same diagram is presented, however, it has been extended with the use of the proposed vision indicator. The application of the disturbance level element marked in the diagram in Fig. 4 allows compensation of visual disturbances, with additional assurance of the fixed conditions of the observed image by the proposed system. Consequently, this can translate into safer operation of the aircraft. The general concept assumes certain features of the proposed system, which, however, do not have to be a determinant:

- the solution should minimally interfere with the installed avionics on the aircraft or the equipment of the ground station (non-invasive solution [20]),
- it can be a mobile solution or a stationary device (eg. integrated with displays in a ground station),
- the hardware concept assumes the use of the system in both classic and unmanned aviation,
- thanks to the possibility of expanding and multilayer decomposition of the output image, the solution allows displaying both the direct image of the environment observed by the image sensor, but also allows it to be integrated with the HUD transparent indicator (Head Up Display).



Fig. 5. Proposed concept in application to UAV; observation camera on UAV (left) and operator's console view (own elaboration)

Integration with HUD or eyepiece index can introduce information about the augmented reality (eg. hazards in the environment, runway lines, type and method of lighting auxiliary landing systems [1, 27, 46]).

The image seen by the transducer, just like the human eye, is just as sensitive to light interference. The difference is that the human eye has a limited and individual adaptation threshold. Depending on the frequency of the interfering signal, the pilot's vision copes with this phenomenon better or worse. In the case of permanent disturbances it may cause temporary blinding. For Gaussian disturbances, with a frequency of periodic changes between 1 Hz and 30 Hz, the pilot, apart from the effect of dimming and lightening, will also see cyclical flickering (caused by, for example, rotary motion of the rotor on the helicopter). The imaging sensor system, armed with the right optics and assisted by the proposed algorithm, can be an effective tool to eliminate these problems. At the beginning, the image is sampled from the transducer and sent as a video stream to the computing computer. Here, the second processing step begins, where the video stream is digitally processed according to a specific algorithm, so that the output can receive an image free of undesirable light effects. The applied algorithm can be additionally equipped with functions forming the so-called augmented reality, introducing synthetic indications to the image [3, 4, 5, 12, 17, 27].

2.2. Hardware structure of the system

The proposed hardware solution of the system can be divided into four parts: optical system, image sensor, computing computer and visualization system (Fig. 6).

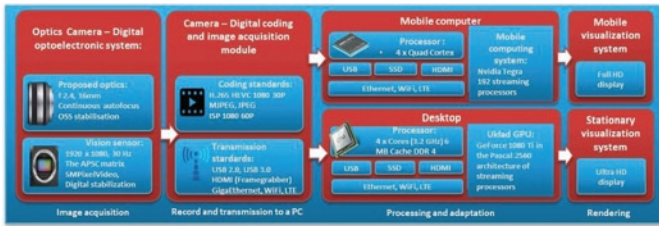


Fig. 6. Diagram of the hardware structure of the proposed solution

The optical system is a lens adapted to work in a different range of light intensity, but typical for observing landscapes. This system should additionally be characterized by a low distortion factor and a wide range of brightness loss at the edges of the image with a variable diaphragm. In our case, the image sensor system is a sensor that ensures (along with the selected optics) a field of view in the range of 90°-120°. The computing system, depending on the application, may be stationary or mobile.

The stationary system is an efficient PC that supports graphic computing. In the case of a mobile system, it is a workstation equipped with an efficient parallel calculation module. On computing computers, it is necessary to place the target system (Windows or Linux) with the developed software for image signal correction installed. The last element is a visualization system, which should be adapted to display the image in the standard Full HD standard and additionally provide the possibility of automatic hardware adjustment of the display brightness to the ambient luminance.

2.3. Image processing algorithms

The schematic diagram of the image processing algorithm is presented in Fig. 7. The characteristic elements of this algorithm are blocks of adaptive interference filtration, where there is a filter that eliminates minor "salt and pepper" disruption, adaptive filter and brightness control of the output image.

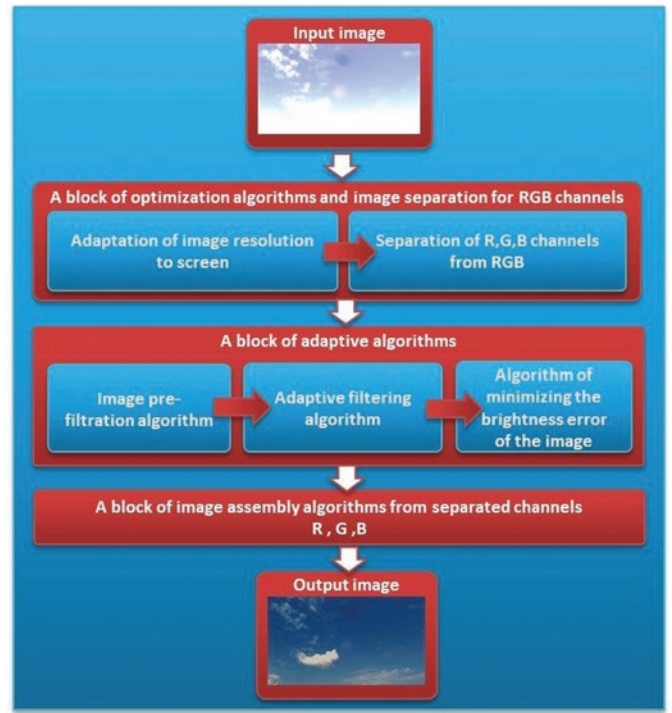


Fig. 7. Schematic diagram of the image processing algorithm

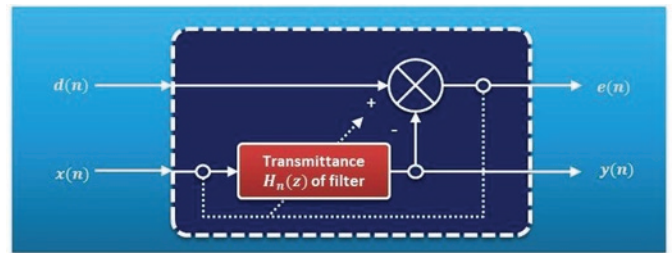


Fig. 8. Adaptive filter structure; d (n) - reference signal, x (n) - filtered signal, e (n) - error signal, y (n) - filtration result

Filter with variable transmittance $H_n(z)$ converts the input signal $x(n)$ so that the resulting signal $y(n)$ has a minimum error with reference to the reference signal $d(n)$. The optimal coefficients selected by the filter change as a function of time. Transmittance $H_n(z)$ for the recursive adaptive filter has the form (1):

$$H_n(z) = \frac{b_0(n) + b_1(n)z^{-1} + b_2(n)z^{-2} + \dots + b_m(n)z^{-M}}{a_1(n)z^{-1} + b_2(n)z^{-2} + \dots + a_n(n)z^{-N} + 1} \quad (1)$$

The output signal $e(n)$, called the error of matching the output signal $y(n)$ to the set input signals $d(n)$ and $x(n)$ is a function of filter coefficients, which can be dependent on the value of signal $y(n)$ (Fig. 8). Depending on the internal configuration of the filter, it can be used for calculations such as:

- model identification,
- inverted modeling,
- prediction of the output signal,
- filtration of the input signal.

From the point of view of applying the adaptive filter to the proposed solution, the structure presented in Fig. 9 seems appropriate. The system structure programmed for interference removal is usually constructed such that the basic input signal is the signal $d(n)$ desired,

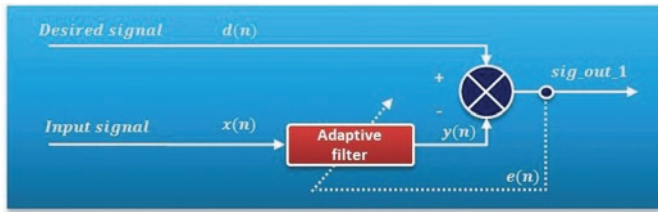


Fig. 9. The structure of the adaptive filter to eliminate interference

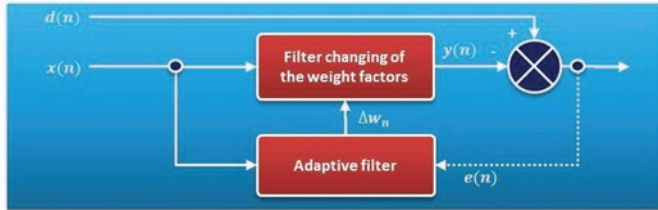


Fig. 10. General conceptual block diagram of the RLS adaptive filter used in the image processing algorithm

the signal $x(n)$ contains interference present in the base signal, the filtered output signal $y(n)$ is subtracted from the desired signal and on this basis the signal $e(n)$ called the error signal is generated, which in turn is used as a signal to select the weighting factors w_n (depending on the type of adaptive algorithm). In the discussed solution, the use of adaptive filtration was proposed on the example of the scheme given in Figure 10. The idea of using a filter using the proposed adaptive algorithm is based on the automatic selection by the weighting algorithm w_n by constantly updating the filter with new data, based on the principle of the so-called autoregressive model with an external input (discrete input-output model for stochastic processes). In the discussed solution $d(n)$ is the standard luminance level of the image, the signal $x(n)$ is the signal representing the current luminance level of individual frames of the input image, $y(n)$ represents the output signal adapted to the standard luminance, with reduced interference (depending on the degree of recursion). The simplified model of such a filter for the system may be general expressed as dependence (2):

$$y(n) = z^{-k}(B(z^{-1}) / A(z^{-1})) + e(n)(1 / A(z^{-1})) \quad (2)$$

where:

- $y(n)$ – output values at time “n”,
- $e(n)$ – vector of the value of the determined error,
- z^{-k} – delay of the signal by “k” moments,
- $z^{-k}(B(z^{-1}) / A(z^{-1}))$ – basic part of the control track,
- $e(n)(1 / A(z^{-1}))$ – stochastic interference.

In the case of a practical application, a simplified expression of (2) given by the formula (3) is used more often:

$$y(n) = \hat{w}^H(n-1)x(n) \quad (3)$$

$x(n)$ – vector containing input values.

The algorithm inside the adaptive filter is to minimize the weight index, which in the general case is defined as (4):

$$\hat{w}(n) = \hat{w}(n-1) + k(n)e(n) \quad (4)$$

$\hat{w}(n)$ – value of the weight vector estimated at the moment “n”.

Vector $k(n)$ it is called the Kalmanian reinforcement and is defined by the formula (5):

$$k(n) = (\lambda^{-1}P(n-1)x(n)) / (1 + \lambda^{-1}x^H(n)P(n-1)x(n)) \quad (5)$$

The record (4) was obtained using the general reinforcement formula (6):

$$k(n) = P(n)x(n-1) \quad (6)$$

The covariance matrix $P(n)$ determined by way of a recursive transformation, where the general record of this matrix is (7):

$$P(n) = \lambda^{-1}[P(n-1) - \frac{P(n-1)x(n-1)x^H(n-1)P(n-1)}{\lambda + x^H(n-1)P(n-1)x(n-1)}] \quad (7)$$

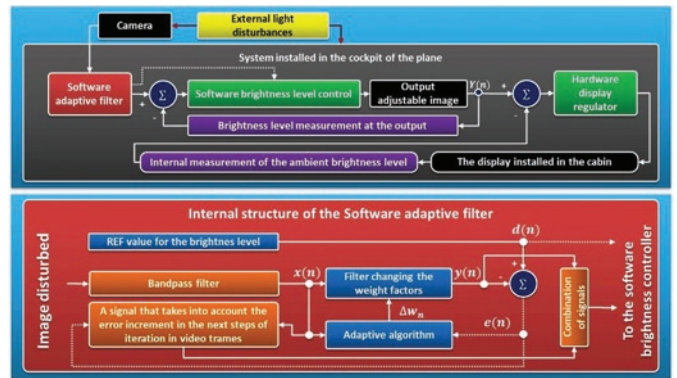


Fig. 11. Scheme of the automatic interference removal and brightness control system of the output image (top), the internal structure of the adaptive filter (on the red block below)

The coefficient λ given in the above formulas is called the forgotten rate and must be predetermined. It can be a value within the range $<0; 1>$ with the indication that the value equal to 1 in the proposed solution means correction at infinity, and 0 the possibility of updating the weight indicator is impossible. Decreasing the value of λ to 0 leads to the limitation of the filter to the current moment of time, without taking into account the states of the previous steps.

Returning to the general structure of the proposed solution, the signal goes to the adaptive system after passing through the bandpass filter. Next, the adaptive system cooperates with the discrete regulator, according to the diagram shown in Fig. 11. This system has an additional reference input and a tracking input that allows dynamically minimize changes in the brightness level of the output image, resulting from changes in the calculated error parameter and weight coefficients of the RLS filter, and consequently the so-called. Kalman reinforcements. During operation, this results in the output of a picture free from interference, but exposed to changes in brightness depending on the amplitude and speed of changes in the brightness of the input image. These changes are mainly influenced by the value of the chosen factor λ .

The programmable brightness level controller introduced into the adaptive system operates based on the 2DOF PID algorithm. An error

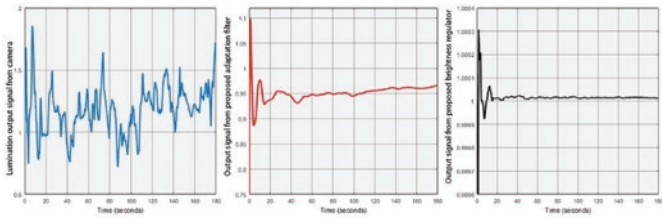


Fig. 12. Disturbed luminance signal (left), output signal $y(n)$ for a system without software brightness controller (central graph) and signal $y(n)$ for a system with a 2DOF PID software controller

signal and a reference value are sent directly to the input from the filter. This regulator stabilizes the signal coming out of the adaptive filter system and minimizes the error of changes in the brightness level of the image in subsequent n -frames relative to the reference value set (Figure 12). This solution makes it possible to reduce interference, and to obtain a relatively constant amplitude of the brightness level of the output image.

3. Results of the study

This chapter presents examples of simulation results. The proposed solution has been tested in the Matlab / Simulink computing environment. The vision system was modeled along with the algorithm for automatic control of the brightness level of the output image, operating in accordance with the structure shown in Figure 11. As a source signal, a video signal recorded by a camera mounted on the hull of an unmanned platform, under normal visibility conditions, with a relatively large range of variation of the average luminance level of the input image between the values 0.0 and 2.5 was used. The value 0.0 means the image is completely darkened, while 2.5 the image is blown. This signal was additionally superimposed by both constant and Gaussian disturbances, with simultaneously variable amplitude and frequency parameters. The presented graphs (Figs 13-18) present three types of signals. The first from the left is the input signal $x(t)$, then the output signal $y(t)$ from the tested system and the regulation error are presented $\varepsilon(t)$ obtained during testing of the system in a simulation environment. Analyzing the presented graphs it can be observed that the output signal from the proposed algorithm works effectively, reducing the interference in the frequency band distinguishable for the human eye. Fig. 13 presents the case of system testing under conditions where the input luminance parameter of the image was changed due to rapid changes in the spatial orientation of the UAV. This test was carried out under specific operating conditions resulting from the low sun position, which is the case when piloting a small and light unmanned aircraft at relatively low altitudes, it has a huge impact on safety. Simulation of similar situations has also shown that the proposed algorithm, regardless of the orientation of the camera relative to a strong light source, allows you to display the image at a constant level of luminance. The results of the tests presented in Fig. 14-15 prove the effectiveness of the algorithm for disturbances related to both the change in the spatial orientation of the UAV (relative to the sun), but also an additional interference that is added to it, integrating (progressing twilight) or differentiating (eg. mechanical jamming of the camera shutter due to overloads or changing thermal conditions). The influence of other types of disturbances is illustrated in Figs. 16-18. They concern the resistance tests of the algorithm to Gaussian interference and 10 Hz shift frequencies (Fig. 16) and 0.1 Hz (Fig. 17). Such a situation may occur, for example, during a spin, in the spinning phase with constant speed. For both a classic airplane and an unmanned aircraft it is possible to obtain an angular speed of up to several hundred degrees per second. A 90° aircraft spin and simultaneous rotations with respect to the x axis, combined with low sun positions, can cause strong pilot sideways distortions of vision in the

pilot or operator. The fourth group of simulations are tests analogous to those presented in Figs. 16-17, with the difference that they were performed with the decreasing and increasing (Fig. 18) spin speed of the aircraft in a spin. Obtained results indicate that this algorithm will be able to deal with disturbances coming from helicopter rotor blades moving at different speeds.

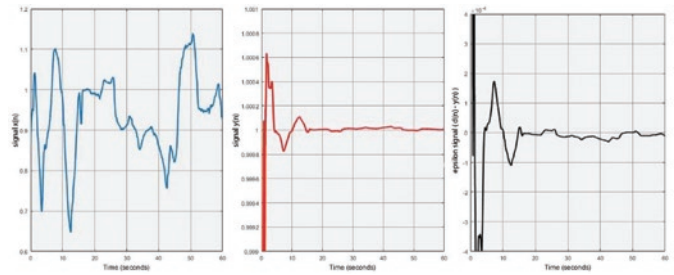


Fig. 13. Characteristics of the adaptive control system during signal processing in free conditions (no additional external interference)

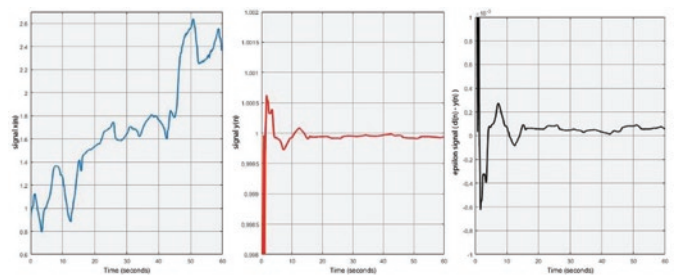


Fig. 14. Characteristics of the system with additionally imposed integral extortion

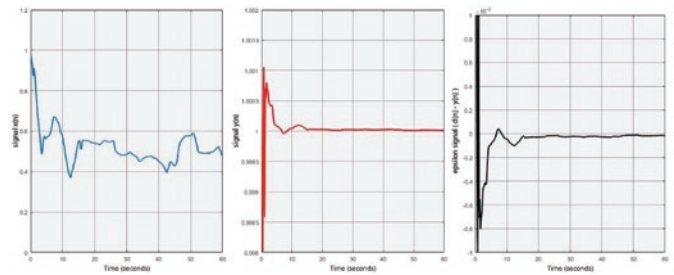


Fig. 15. Output characteristics with additionally imposed forcing of a differentiating character

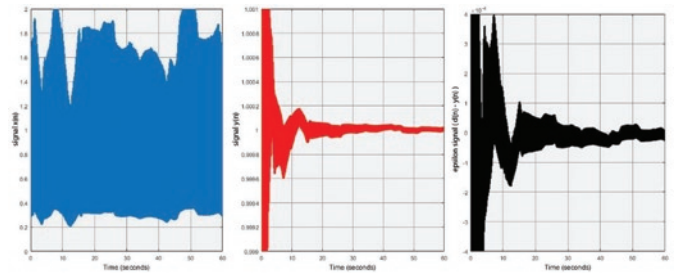


Fig. 16. Output characteristics of the system with additionally imposed Gaussian forcing with a natural frequency of 10 Hz

Based on the presented time characteristics, it can be observed that the output signal from the proposed brightness control system decreases and eventually the output signal deviation drops to zero. Due to the short nature of the results presented here, the authors sought to show the effectiveness of the proposed solution algorithm for the characteristic variation of input signal interference, usually found in

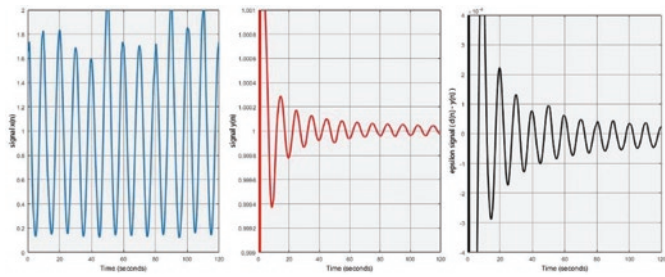


Fig. 17. Output characteristics of the system with additionally imposed Gaussian forcing with an own frequency of 0.1 Hz

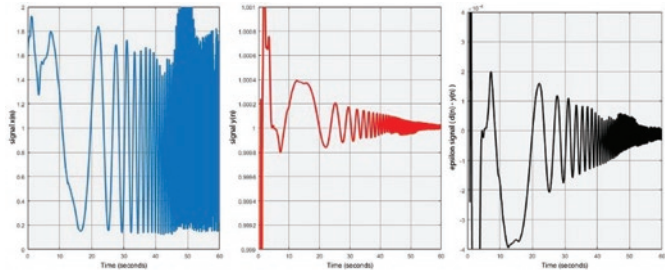


Fig. 18. The output characteristics of the system with additionally imposed gaussian forcing of variable amplitude and increasing natural frequency in the range from 0.01 Hz to 10 Hz.

real aircraft operation conditions. Fig. 19 presents images obtained during the operation of the algorithm with fixed luminance parameters. Under real conditions, changes in luminance will result not only from changes in the spatial orientation of the aircraft, but also from changes in the time of day. In this picture, the input image is visible on the left, and the resulting image from the proposed system on the right. The simulations were carried out for one test image, the luminance of which was changed from 0.25 (characteristic of underexposed image) to 2.5 (overexposed image).



Fig. 19. Input images (left) with luminance value (from above, respectively: 0.25, 1.5, 2.5) and the output image (right)

4. Final conclusions

The proposed solution, although it concerns aviation, is an interdisciplinary solution. It can also be used in other areas of transport (eg. in the automotive industry). The presented concept is based on the processing of signals and control theory, but the article has been

enriched by aspects related to the theory of the human factor and is connected with aircraft operation problems in general.

The problem of glare occurs in aviation when flying in variable weather conditions and during the change of time of day (sunrises and sunsets). Such conditions have been simulated during research conducted using actual recordings. In the presented time characteristics, it can be observed that the output signal from the proposed image brightness control system stabilizes at the expected luminance value of 1. This happens both in the case of continuous disturbances, such as occur during a typical solar glare occurring during the flight with the “sun” course, as well as in the case of disturbances of a variable nature, caused by sunlight piercing through clouds or resulting from sudden changes in the spatial orientation of the aircraft. Such phenomena may be particularly troublesome during operation in atypical flight conditions connected, for example, with aerobatics or control of a highly manoeuvrable aircraft, where the object changes its position relative to the sun (and other light sources) in an abrupt manner. The proposed system quickly eliminates in such situations temporary oscillations of the light intensity to values deviating from the standard luminance equal to 1.0 by no more than $\pm 1 \times 10^{-4}$. If the pilot observes such an output image, the light oscillation is unnoticeable. It should also be remembered that the proposed final solution still has a hardware adjuster for adjusting the brightness level of the display, depending on the level of ambient luminance.

Research carried out at present by research teams around the world in the field of vehicle operation in the field of broadly understood transport has been turning in recent years towards the use of optical and vision methods [8, 20, 21, 33, 39, 44]. The presented solution has high development chances. In the future this system will be integrated with the pilot-assistant system developed by the authors. It will be tested during operation in selected phases of flight. This solution can be used both to improve the precision of maneuvers performed manually by the pilot-operator, as well as to support the automatic detection of objects (intruders) that could pose a potential threat to the aircraft. The tests and research carried out indicate also the possibility of using the developed solution to avoid glare the staff through the light of an amateur laser. The proposed solution may support further interdisciplinary research on the improvement of observation conditions conducted by the pilot or UAV operator during the operation of the aircraft.

References

1. Abramov A, Bayer C, Heller C. A flexible modeling approach for robust multi-lane road estimation, IEEE Intelligent Vehicles Symposium (IV), 10.1109/IVS.2017.7995904, Los Angeles, CA, 2017, <https://doi.org/10.1109/IVS.2017.7995904>.
2. Aircraft Spruce, http://www.aircraftspruce.com/catalog/graphics/notinuse/RV-10Rosen_B.jpg, access: 2018.07.19.
3. Akopdjaniyan Y, Machikhin A, Bilanchuk V, Drynkin V, Falkov E, Tsareva T, Fomenko A. Flight study of on-board enhanced vision system for all-weather aircraft landing, 20th International Symposium on Atmospheric and Ocean Optics: Atmospheric Physics 2014; 9292: 92920X.
4. Arthur J, Kramer L, Bailey R. Flight test comparison between enhanced vision (FLIR) and synthetic vision systems. *Enhanced and Synthetic Vision* 2005; 5802: 25-37, <https://doi.org/10.1117/12.604363>.
5. Basmadji F, Gruszecki J, Kordos D, Rzucidlo P. Development of ground station for a terrain observer-hardware in the loop simulations. AIAA Modeling and Simulation Technologies Conference 2012; 4629, <https://doi.org/10.2514/6.2012-4629>.
6. Basmadji F, Gruszecki J, Rzucidlo P. Prediction, Analysis and Modeling of Human Performance. Digital Human Modeling for Design and Engineering Conference and Exhibition, Gothenburg - Sweden 2009; SAE Technical Paper 2009-01-2297.
7. Beier K, Gemperlein H. Simulation of infrared detection range at fog conditions for Enhanced Vision Systems in civil aviation. *Aerospace Science and Technology* 2004; 8(1): 63-71, <https://doi.org/10.1016/j.ast.2003.09.002>.
8. Boden F, et al. Editorial for the special feature on Advanced In-flight Measurement Techniques AIM2. *Measurement Science and Technology* 2017; 28.4: 040101.
9. Cernasov N. Automatic glare reduction system for vehicles. Patent application US20090204291A1 2009.
10. Ciecinski P, Pieniążek J, Rzucidlo P., Tomczyk A. Modyfikacja charakterystyk systemu pośredniego sterowania samolotem z wykorzystaniem interfejsów człowiek-maszyna, *Sieć Naukowa Aeronautica Integra*. *Journal of Aeronautica Integra* 2008; 2(4): 29-36.
11. Engerstrom L, Samuelsson A. Exploring sun visor concepts, Department of Technology Management and Economics Division of Entrepreneurship and Strategy, Chalmers University of Technology. Gothenburg, Sweden 2016; Report No. E 2016:102
12. Foyle D, Ahumada A, Larimer J, Sweet B. Enhanced/Synthetic Vision Systems: Human Factors Research and Implications for Future Systems, 1992; SAE Technical Paper 921968, <https://doi.org/10.4271/921968>.
13. Gruszecki J. [red] Wybrane zagadnienia awioniki, Kijor K., Rzucidlo P., Szpunar R., *Integracja systemów syntetycznej i wzmacnionej wizji*, Oficyna Wydawnicza Politechniki Rzeszowskiej, Rzeszów 2011, 61-70.
14. Gruszecki J, Rogalski T, Nowak D. Precision of Pilotage as a Function of Pilot Information Workload. AIAA Modeling and Simulation Technologies Conference, Minneapolis 2012; AIAA-2012-4492, <https://doi.org/10.2514/6.2012-4492>.
15. Gruszecki J, Rzucidlo P. Simplified Informatics Model of Pilot-Operator and Prediction of Human Performance. AIAA Modeling and Simulation Technologies Conference and Exhibit, Honolulu, Hawaii 2008; AIAA-2008-7110.
16. Gruszecki J, Tomczyk A, Rzucidlo P, Dołęga B, Kopecki G, Pieniążek J, Rogalski T. Opracowanie technologii oraz stanowiska do optymalizacji interfejsu człowiek-maszyna w kokpitach wojskowych statków powietrznych. Wydawnictwo Instytutu Technicznego Wojsk Lotniczych, Warszawa 2007.
17. Hines G, Rahman Z, Jobson D, Woodell G, Harrah S, Real-time enhanced vision system, *Proc. SPIE* 5802, *Enhanced and Synthetic Vision*, 2005, <https://doi.org/10.1117/12.603656>.
18. Kashyap S K, Naidu V P S, & Shanthakumar N. Development of Data Acquisition Systems for EVS Flight Experiments, *Control and Data Fusion e-Journal: CADFEJL* 2017; 1 (1): 31-36.
19. Kim J, Shin H. *Algorithm & SoC Design for Automotive Vision Systems*, Springer Netherlands, 2014, <https://doi.org/10.1007/978-94-017-9075-8>.
20. Kopecki G, Rzucidlo P. Integration of optical measurement methods with flight parameter measurement systems, *Measurement Science and Technology*, 2016; 27(5): 054003, <https://doi.org/10.1088/0957-0233/27/5/054003>.
21. Kucaba-Pietal A, Stasiński P, Politz Ch, Roloff Ch, Boden F, Jentink H, de Grot K, Szumski M, Valla M, Póltora P, Szczerba P, James S, Kirmse T, Weikert T. AIM2 Advanced Flight Testing Work-shop. Norderstedt: BOD, 2013.
22. Maier M, Moisel J, Herold F. Multibeam Headlights in the Mercedes-Benz CLS-Class. *ATZworldwide* 2015; 117(2): 4–9, <https://doi.org/10.1007/s38311-015-0156-0>.
23. Moisel J, Ackermann R, Griesinger M. Adaptive Headlights Utilizing LED Arrays. *Proceedings of the Int. Symposium on Automotive Lighting (ISAL) Darmstadt*, 2009; 287–296.
24. Naidu V, Rao N, Girija G. Enhanced and Synthetic Vision for Remotely Piloted Vehicles, 2011.
25. Naidu V P S, Rao P N, Kashyap S K, Shanthakumar N, & Girija G. Experimental study with enhanced vision system prototype unit. In *Image Information Processing (ICIIP)*, 2011 International Conference on (pp. 1-5). IEEE.
26. Nakagawara V, Wood K, Montgomery R. Laser exposure incidents: pilot ocular health and aviation safety issues. *Optometry-Journal of the American Optometric Association* 2008; 79(9): 518-524, <https://doi.org/10.1016/j.optm.2007.08.022>.
27. Oszust M, Kapuscinski T, Warchol D, Wysocki M, Rogalski T, Pieniążek J, Kopecki G, Ciecinski P, Rzucidlo P. A vision-based method for supporting autonomous aircraft landing, *Aircraft Engineering and Aerospace Technology*, DOI: AEAT-11-2017-0250 (accepted for publication).
28. Pencikowski P, Low-cost vehicle-mounted enhanced vision system comprised of a laser illuminator and range-gated camera. *Enhanced and Synthetic Vision* 1996; 2736, <https://doi.org/10.1117/12.241036>.
29. Pieniążek J. Adaptation of the display dynamics for monitoring of controlled dynamical processes. *Human System Interactions (HSI)*, 3rd International Conference on Human System Interaction, Rzeszów 2010, <https://doi.org/10.1109/HSI.2010.5514493>.
30. Pieniążek J. Kształtowanie współpracy człowieka z lotniczymi systemami sterowania, Oficyna Wydawnicza Politechniki Rzeszowskiej, Rzeszów 2014.
31. PKBWL Raport wstępny o wypadku (poważnym incydencie) lotniczym 338/14, Katowice 2014.
32. Polak G. Operational and technological directions for Unmanned Aircraft Systems development. *Security and Defence Quarterly* 2018; 1(18): 57-74, <https://doi.org/10.5604/01.3001.0011.8327>.
33. Politz C, Lawson N J, Konrath R, Agocs J, & Schröder A. Development of Particle Image Velocimetry for In-Flight Flow Measurement. In *Advanced In-Flight Measurement Techniques* 2013: 269-289, https://doi.org/10.1007/978-3-642-34738-2_16.

34. RAM Universal Sun Visor with Suction Cup Mount, <http://www.mypilotstore.com/mypilotstore/sep/9989>, access: 2018.07.19.
35. Rash C, Manning S. For Pilots, sunglasses are Essential in Vision Protection Human Factors & Aviation Medicine 2002; 49(4):1-8.
36. Rash C E, McLean W E, Mozo B T, Licina J R, & McEntire B J. Human factors and performance concerns for the design of helmet-mounted displays. In RTO HFM symposium on current aeromedical issues in rotary wing operation 1999.
37. Reichl M, Intelligente LED-Scheinwerfer für mehr Sicherheit. <http://www.photonikforschung.de/service/aktuellnachrichten/detailseite/archive/2013/05/15/article/intelligente-led-scheinwerfer-fuer-mehr-sicherheit>, access: 2018.07.26.
38. Rozporządzenie (WE) nr 1899/2006 Parlamentu Europejskiego i Rady z dnia 12 grudnia 2006 r. zmieniające rozporządzenie Rady (EWG) nr 3922/91 w sprawie harmonizacji wymagań technicznych i procedur administracyjnych w dziedzinie lotnictwa cywilnego.
39. Rzucidło P, Kopecki G H, deGroot K, Kucaba-Pietal A, Smusz R, Szewczyk M, Szumski M. Data acquisition system for PW-6U in flight boundary layer mapping, Aircraft Engineering and Aerospace Technology, 2016; 88(4):572 – 579, <https://doi.org/10.1108/AEAT-12-2014-0215>.
40. Sánchez-Tena M, Alvarez-Peregrina C, Valbuena-Iglesias M, Palomera P. Optical Illusions and Spatial Disorientation in Aviation Pilots. Journal of medical systems 2018; 42(5): 79, <https://doi.org/10.1007/s10916-018-0935-4>.
41. Sasim B. Elementy ergonomii kabin samolotów wojskowych, Wydawnictwo Instytutu Technicznego Wojsk Lotniczych, Warszawa 2009
42. Stewart K. Podręcznik pilota szybowcowego – praktyka, Wydanie I, 2015.
43. Szczepański C. Method of Optimizing the Human-Machine Interface at Military Aircraft. AIAA Modeling and Simulation Technologies Conference, Chicago, IL 2009; AIAA-2009-5923, <https://doi.org/10.2514/6.2009-5923>.
44. Szewczyk M, Smusz R, de Groot K, Meyer J, Kucaba-Pietal A, Rzucidło P. In-flight investigations of the unsteady behaviour of the boundary layer with infrared thermography. Measurement Science and Technology 2017; 28(4): 044002, <https://doi.org/10.1088/1361-6501/aa529c>.
45. Tutunea D, Dima A, Bica M, Buculei M. The design of sun visors for automotive industry. Annals of the University of Oradea. Fascicle of Management and Technological Engineering 2014; XXIII(XIII): 124-127.
46. Wilson J, Zimmerman K, Schwab D, Oldham M, Stockwell R. U.S. Patent No. 7,525,448. Washington, DC: U.S. Patent and Trademark Office 2009.
47. Yechezkal E. Enhanced vision for driving, Patent No.: US 7,199,767 B2, 2007.
48. Yuter S. Vehicle glare reducing systems, Patent application 20120303214 2012.
49. Zuse K. Fotoelektrisch durch Gegenlicht steuerbare Beleuchtungsvorrichtung. German Patent No. 1190413, 1958.

Piotr SZCZERBA
Paweł RZUCIDŁO
Zygmunt SZCZERBA
Grzegorz DRUPKA

Rzeszów University of Technology,
Faculty of Mechanical Engineering and Aeronautics
al. Powstańców Warszawy 12, 35-959 Rzeszów, Poland

E-mail: psz@prz.edu.pl, pawelrz@prz.edu.pl,
zygszcze@prz.edu.pl, g.drupka@prz.edu.pl
